# Laser-induced anti-Stokes resonance Raman scattering: Probe for energy transfer in $F$-center–$CN^-$-molecule defect pairs in CsCl

K. T. Tsen and G. Halama
*Physics Department, Arizona State University, Tempe, Arizona 85287*

Fritz Lüty
*Physics Department, University of Utah, Salt Lake City, Utah 84112*
(Received 26 May 1987)

Optical excitation of the two electronic absorption bands of $F$-center–$CN^-$ defect pairs in CsCl creates a highly efficient electronic to vibrational ($e$-$v$) energy transfer process, characterized by rapid nonradiative relaxation of the $F$ electron in contrast to a slowly cascading sequence of fluorescence transitions between the six lowest excited $CN^-$ vibrational states. This behavior allows, by pumping with the same laser beam, to both populate nonequilibrium $CN^-$ vibrational states and to probe their existence and physical properties by anti-Stokes resonance Raman scattering. Experiments with this technique were performed, testing the temperature, wavelength, and intensity dependence of the anti-Stokes Raman spectra and their polarization. Comparison with the earlier vibrational emission results show close agreement for low-$CN^-$-doped crystals, but pronounced differences for higher-doped crystals, in which vibrational ($v$-$v$) energy transfer from the $F_H(CN^-)$ centers into the free $CN^-$ defect system occurs. These results provide the basis for using pulsed anti-Stokes Raman spectroscopy as a viable probe for our planned time-resolution studies of the $e$-$v$ and $v$-$v$ transfer in these systems.

## I. INTRODUCTION

Besides being the simplest $O_h$ symmetry electronic defect in ionic crystals, the $F$ center (an electron bound to an anion vacancy) is the most versatile and easily movable "building block" which can be used for successful association to other point defects. The various formed "*F aggregate centers*" of reduced local symmetry, changed wave functions, and electron-phonon coupling still share as a common feature with their $F$-center origin highly efficient, spectrally broad, and Stokes-shifted electronic emission bands. Several of these $F$ aggregate centers have gained significance as solid-state electronic systems capable of tunable near-ir laser emission.

In view of the long history and great variety of atomic defects as partners for $F$-center association it is amazing that simple molecular defects, like $CN^-$ or $OH^-$ ions, have been employed for this purpose only very recently. These new $F_H(CN^-)$ or $F_H(OH^-)$ defect pairs[1,2] produce under visible light excitation *electron-vibrational (e-v) energy transfer* from the excited $F$ electron into localized vibrational modes of the attached molecular ion. The nature and strength of the $e$-$v$ transfer process and its effect on the radiative or nonradiative decay of the excited $F$ electron and on the vibrational excitation of the attached molecule varies strongly with both host material and molecule ($CN^-$ or $OH^-$). Intense studies are currently under way, with the aim to clarify and understand the kinetics and physical mechanism of these $e$-$v$ coupling and transfer processes and their trend with hosts and molecules.[3,4]

We apply in this work a new optical technique to the best studied system,[5] which presently carries the greatest potential for scientific insight and potential for laser application:[6] *the F-center–$CN^-$-molecule pair in CsCl.* Figure 1 illustrates and summarizes the structural model, wave functions, electronic and $CN^-$ vibrational levels (in a common energy scale), and the considered transition and exchange processes of this defect pair. The closest possible attachment [next-nearest neighbor (NNN)] of the $CN^-$ in a $\langle 100 \rangle$ direction splits the single $1s \rightarrow 2p$ $F$-band transition into two absorptions $F_H(1)$ and $F_H(2)$, polarized parallel and perpendicular to the $F$-center–$CN^-$ pair axis. Optical excitation in both of these absorptions produces the same highly efficient energy transfer from the excited electron into vibrational modes of the neighboring $CN^-$ molecule. Though the exact mechanism of these processes is not yet understood, three important experimental consequences have been established [Fig. 1(a)]: (i) *rapid nonradiative relaxation of the excited electron into its ground state* (dashed line); this electronic decay is caused by (ii) *e-v energy transfer into the $CN^-$ stretching mode* (double-line arrow), creating a distribution of populations in the various vibrational levels of the $CN^-$ molecule. The distribution is indicated schematically by a dotted block diagram, showing that the maximum probability for energy transfer occurs at $\sim 1$ eV into the $v=4$ state of the $CN^-$ molecule. (iii) If "left alone" after this $e$-$v$ transfer, the $CN^-$ excitations decay by a cascade of $\Delta v = 1$ *vibrational fluorescence processes* on a msec timescale between the six lowest vibrational levels.[5,6] This leads to a full vibrational relaxation only after $\sim 20$ msec.

Different from all $F$ and $F$ aggregate centers in ionic crystals, optical excitation of this $F_H$ center creates a defect with an excited electron which returns extremely

 

quickly into the ground state, while its transferred energy persists for a much longer time period in highly excited states of localized vibrations of a neighboring $CN^-$ molecule. This provides the basis for our planned experiments, illustrated in Fig. 1(b). After the first excitation cycle (a), a quickly repeated re-excitation of the $F$ electron can create an anti-Stokes resonance Raman process (b), which will reflect in the spectral structure and strength of $\Delta v=1$ transitions, the populations in the various $CN^-$ vibrational levels and the strength of the Raman coupling between the $F$ electron and these $CN^-$ molecules. With the recent advance of ultrashort visible-light laser sources, detectors, and time-delay techniques, this Raman approach can become an ideal tool for studying the short-time kinetics of the $e$-$v$ transfer processes in $F$-center—molecular-defect complexes in ionic crystals—highly advantageously in time resolution to ir vibrational fluorescence measurements.

## II. EXPERIMENTAL TECHNIQUE AND CRYSTAL SAMPLES

We used in our experiments the same beam of laser radiation of wavelengths either at $\lambda=532$, 575, or 650 nm, to simultaneously generate the nonequilibrium vibrational $CN^-$ population through the excitation of the $F_H$ center electron [Fig. 1(a)], and for exciting *in situ* 90° resonance Raman scattering [Fig. 1(b)]. The 532-nm radiation is generated in 60-ps pulses from the second harmonic of a cw mode-locked yttrium aluminum garnet (YAG) laser, while 575- and 650-nm radiation is produced, in 3-ps pulses, by Rhodamin 6G and DCM dye lasers, synchronously pumped by the frequency-doubled cw mode-locked YAG laser. The laser beam is focused on the crystal into a channel of $\sim 200$ $\mu$m diameter, pumping a volume of $\sim 2\times 10^{-4}$ cm$^3$. For a time-averaged pump power of 200 mW, each pulse (with repetition rate of 76 MHz) consisted of about $7\times 10^9$ photons, thus creating in the crystal an average photon flux of $5.3\times 10^{17}$ photons/sec. The anti-Stokes Raman scattered light was analyzed with a Spex double-grating monochromator, S-20 photomultipiler, and a photon-counting system. The experimental data were taken by a computer-controlled Raman system and at various temperatures with the help of a Janis supervaritemp dewar flask. The slit widths were chosen in such a way that the spectral resolution was about 10 cm$^{-1}$. The samples of CsCl, containing $7\times 10^{-4}$ and $6\times 10^{-3}$ mole ratios of $CN^-$, were grown by the Bridgeman technique in the Utah Crystal Growth Laboratory. The properly cut and polished samples were quenched from $T=250$ °C (to remove unwanted $F$ aggregate centers) and carefully transferred in the dark at room temperature into the dewar flask. At $T\approx 170$ K the $F$ centers were aggregated into $F_H(CN^-)$ by exposure of the crystal to flashlight for about 15 min.

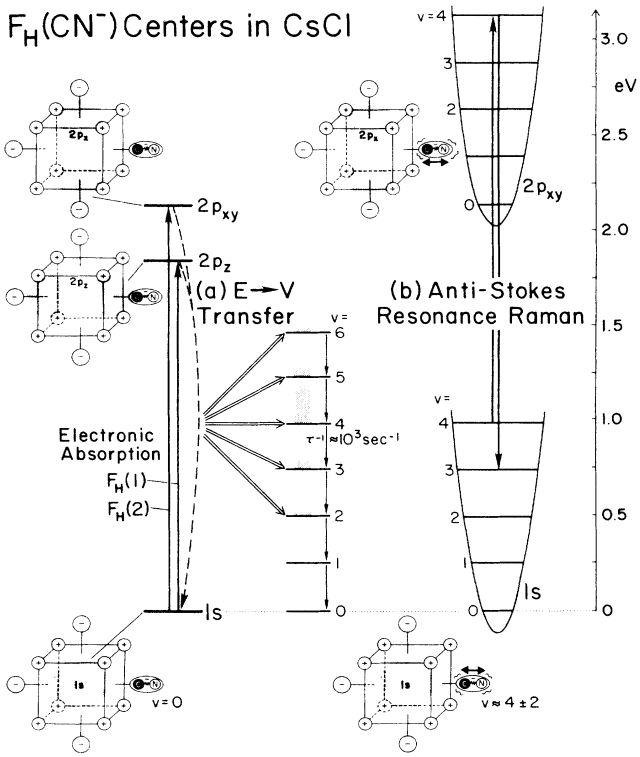


FIG. 1. Structural model, electronic wave functions and eigenstates, and $CN^-$ vibrational levels of $F_H(CN^-)$ defect pairs in CsCl, plotted in a common energy scale for two types of transition processes: (a) electronic $F_H(1)$ and $F_H(2)$ absorptions, producing $e$-$v$ transfer and subsequent $\Delta v=1$ fluorescence transitions among the six lowest $CN^-$ vibrational states; and (b) anti-Stokes resonance Raman process of an $F_H$ center in the $v=4$ $CN^-$ vibrational state [excited in its electronic $F_H(2)$ absorption].

## III. EXPERIMENTAL DATA AND DISCUSSION

All measurements reported in Figs. 2–4 refer to $F(CN^-)$ defects in CsCl crystals doped with rather low ($7\times 10^{-4}$) $CN^-$ concentration. Figure 2(a) shows anti-Stokes Raman spectra measured at 20 K under pumping at two different laser wavelengths $\lambda=532$ and 575 nm. We observe that the intensity of the Raman signal increases by about one order of magnitude when changing the pumping wavelength from 532 to 575 nm. As 532 nm lies at the high energy tail and 575 nm close to the maximum of the $F_H(2)$ absorption band, the observed signal increase is a combination of rising absorption (i.e., pumping) strength and resonance enhancement of the Raman effect, both expected to peak at the $F_H(2)$ band maximum. As Fig. 2(a) shows, the relative intensity among the six anti-Stokes Raman peaks changes very little with different laser excitation.

Comparison of these Raman spectra with the vibrational emission spectra[7] [Fig. 2(b)], shows an amazingly good coincidence in the spectral position of the six well-defined lines observed with the two techniques. As the almost-equal line separation of $\sim 25$ cm$^{-1}$ corresponds to the anharmonicity shift among the $CN^-$ oscillator states, we interpret the six lines as the $\Delta v=1$ Raman and ir transitions among the seven lowest-energy $CN^-$ vibrational states ($v=0$–6), as indicated by dashed lines in

Fig. 2. The relative intensity of the six observed lines reflects the population obtained under optical pumping in the different $CN^-$ states. Both ir (Refs. 5–7) and the new Raman data show clearly that the strongest *e-v* transfer takes place into the $v=4$ state and creates the highest population in this state [as schematically illustrated in Fig. 1(a)]. The slight difference in the relative intensity variation among the six lines between the Raman and ir data is caused by very different pump rates used in both techniques and by special phase effects from the chopped light lock-in amplifier detection method used in the ir experiment. The anti-Stokes Raman measurements are free from this, and therefore reflect by the relative intensity of the six lines directly the relative population of the excited $CN^-$ states.

The most pronounced difference between the ir and Raman data in Fig. 2 is the appearance of two extra ir lines of the high-energy end of the spectrum. These lines originate from the $v=2\rightarrow1$ and $1\rightarrow0$ transitions of isolated $CN^-$ defects, which have about 11 $cm^{-1}$ higher energy compared to the corresponding $CN^-$ transitions in the $F_H$ complex.[5] For any reasonably high $CN^-$ concentration, $CN^-$ excitations in an $F_H$ center complex can transfer—with the help of thermal activation—the vibrational energy into the abundant isolated $CN^-$ defect system (particularly at the lower $v$ levels, which better match in energy), and appear as isolated $CN^-$ defect vibrational emission. Though the same *v-v* transfer process should occur in the optical pumping cycle preceding the Raman experiment, they should not appear under $F_H$ center reexcitation as a resonance anti-Stokes Raman response. We see indeed in Fig. 1(a), that under $\lambda=575$ nm excitation in the maximum of the $F_H(2)$ absorption, no trace of this isolated $CN^-$ defect signal shows up. In the (ten times weaker) resonance Raman spectrum excited at 532 nm, however, a small signal of the "free" $CN^-$ $1\rightarrow0$ transition is detectable. Two interpretations for this behavior are possible.

(a) The isolated $CN^-$ defects, excited by the $F_H$ center pumping cycle and *v-v* energy transfer, appear in our measurements as a weak off-resonance anti-Stokes Raman signal.

(b) 532 nm lies on the high-energy side of the $F_H(2)$ band in a spectral range, where higher electronic absorption transitions ("*K* band") (Ref. 8) overlap the $F_H(2)$ band in absorption. Tuning the excitation into this range produces in pure *F* centers pronounced spectral changes in the normal first-order resonance Raman scattering[9] which can be explained by the diffuse nature of the higher excited states.[10] In our case these may couple to $CN^-$ defects, which are neither totally attached to or isolated from the *F* center, but are located in its very close neighborhood.

The measurement in Fig. 3 sheds more light on this open question. We measured here, for the same crystal as used in Fig. 2, the temperature variation of the anti-

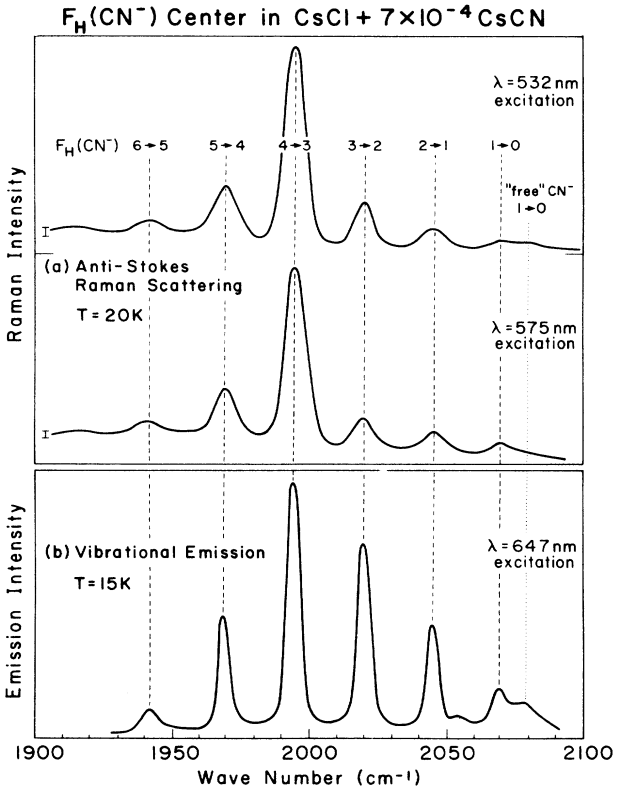


FIG. 2. Comparison of Raman and ir emission processes for $F_H(CN^-)$ centers in low-doped CsCl with $7\times10^{-4}$ $CN^-$. (a) Anti-Stokes Raman spectra obtained at $T=20$ K under $\lambda=532$ and 575-nm excitation. (b) Vibrational emission spectrum, obtained at $T=15$ K under $\lambda=647$ nm excitation.

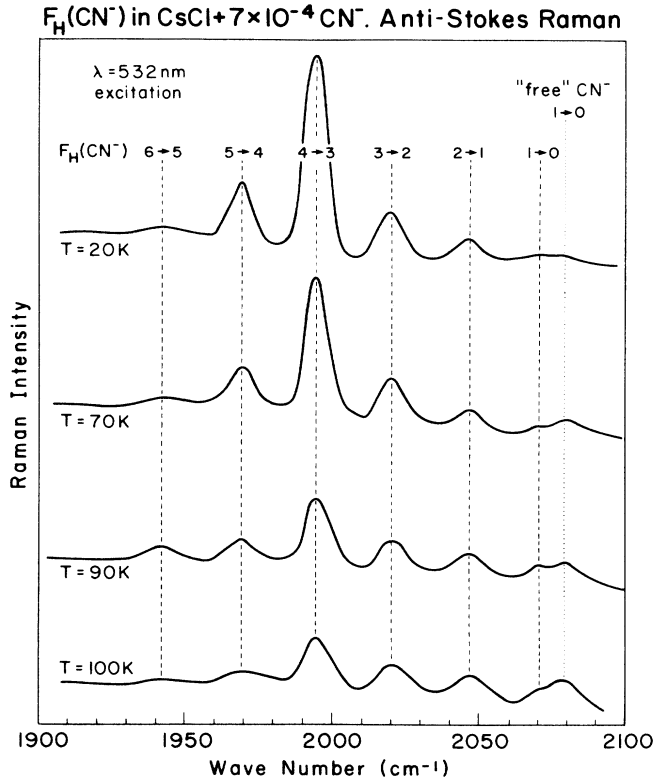


FIG. 3. Temperature dependence of anti-Stokes Raman spectra, obtained under 532-nm excitation of $F_H(CN^-)$ centers in CsCl with $7\times10^{-4}$ $CN^-$.

Stokes Raman spectrum under $\lambda=532$ nm excitation. As the temperature increases, firstly the six $CN^-$ Raman lines of the $F_H(CN^-)$ complex reduce gradually in intensity, with more reduction in the transitions between the high compared to the low vibrational levels. Secondly, the very weak $v=1\rightarrow 0$ signal of the "free" $CN^-$ increases appreciably with temperature. Both observations are in agreement with the ir emission results.[5] They show that thermally activated $v$-$v$ energy transfer into the "free" $CN^-$ system becomes more efficient with increasing temperature, and is observable with the anti-Stokes Raman technique too. However, we can not yet decide from these results which of the above interpretations (a) or (b) for an off- or on-resonance Raman effect is the valid one.

In Fig. 4 we show for the same crystal under $\lambda=575$ nm excitation how the intensity of the six $F_H(CN^-)$ Raman transitions change under variation of the average laser power. This is interesting because the anti-Stokes Raman effect is based on *two* laser excitation processes: *pumping* to create an excited $CN^-$ population [Fig. 1(a)] and *probing* for its Raman response [Fig. 1(b)]—both of them in principle linearly depending on the laser intensity. In practice, however, two experimental behaviors can be expected, depending on the question if the average time $\Delta t_{exc}$ between successive excitations of the same $F_H(CN^-)$ center is long or short compared to the $CN^-$ vibrational relaxation time $\tau_{rel}$ in the $F_H(CN^-)$ complex.

(a) If $\Delta t_{exc} > \tau_{rel}$ the achieved excited $CN^-$ population (and the Raman response as well), depends linearly on the pump intensity, we expect *quadratic* dependence of the Raman intensity on the pump power.

(b) If $\Delta t_{exc} < \tau_{rel}$ the achieved excited $CN^-$ population will essentially be (and remain) saturated, and we expect a linear dependence based only on the linear intensity dependence of the Raman response.

Our obtained results in Fig. 4 are very clear: the lower level transitions ($1\rightarrow 0$, $2\rightarrow 1$, $3\rightarrow 2$) show within experimental accuracy a strictly linear dependence $I \propto P^{1.0}$, while the higher transitions ($4\rightarrow 3$, $5\rightarrow 4$) show a slightly higher ($I \propto P^{1.2}$) power-law dependence. These results are well understandable: For our used $F_H$ center concentration of $\sim 5\times 10^{16}$ $cm^{-3}$ we estimate (based on the average photon flux and illuminated crystal volume mentioned in Sec. II) for the 20–200-mW power range of Fig. 4 average values of $\Delta t_{exc}$ in the $10^{-2}$–$10^{-1}$-msec range. For the lower $CN^-$ vibrational levels this $\Delta t_{exc}$ is much smaller than $\tau_{rel}$ ($\approx 10$ msec), so that total population saturation and a linear dependence is expected. For the higher levels the relaxation time decreases into the 1-msec range,[5] so that minor depopulation between optical pump and probing excitation can occur. This produces the slightly higher than linear dependence which we observe in Fig. 4.

In Fig. 5 we make an important change, increasing the concentration of free $CN^-$ defects by about one order of

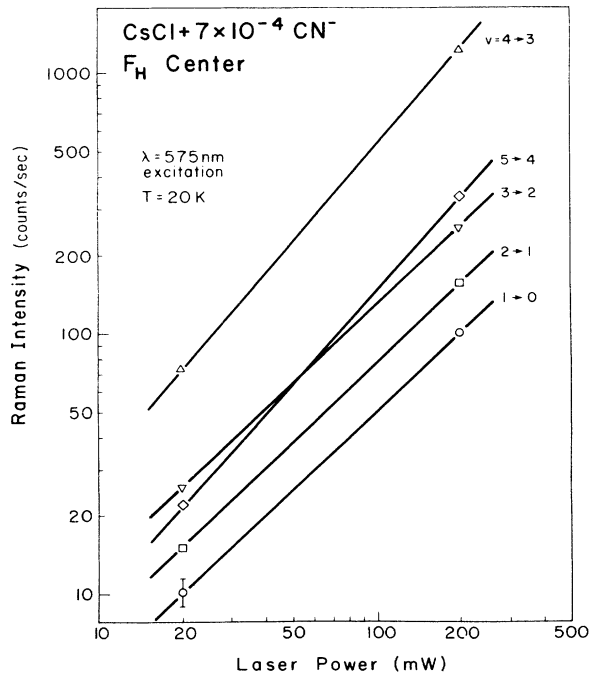


FIG. 4. Anti-Stokes Raman intensity of the five $\Delta v=1$ transitions as a function of averaged laser power in a double logarithmic plot, obtained at 20 K under $\lambda=575$ nm excitation.

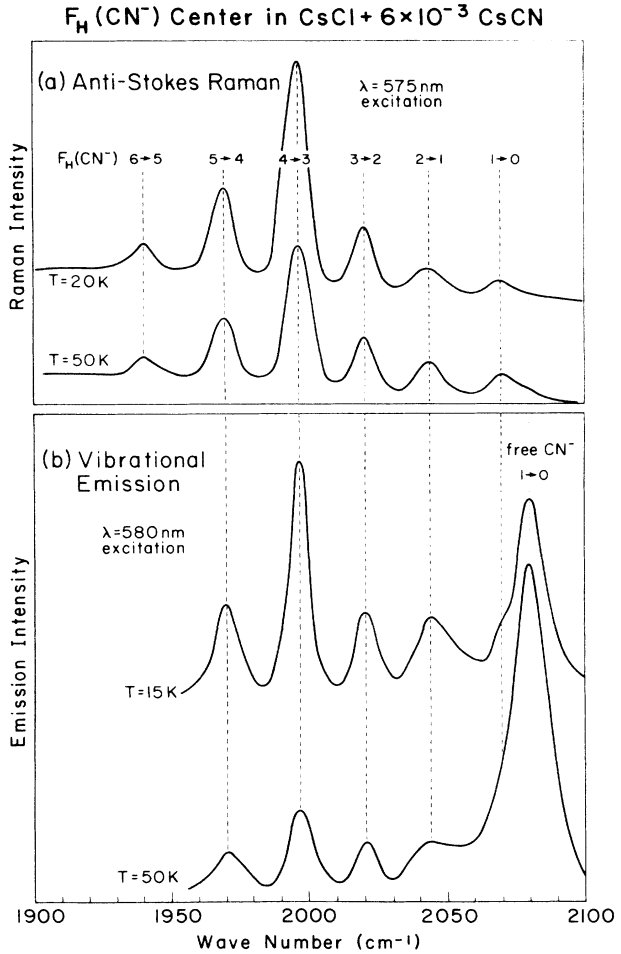


FIG. 5. Comparison of anti-Stokes Raman (a) and vibrational emission (b) spectra, both measured at two low temperatures for $F_H(CN^-)$ defects in higher-doped CsCl with $6\times 10^{-3}$ $CN^-$.

magnitude (to $6\times10^{-3}$ mol parts), but keeping the concentration of $F_H(CN^-)$ complexes the same compared to the earlier measurements ($\sim3\times10^{-6}$). This variation should cause a strong increase in the efficiency of vibrational energy $v$-$v$ transfer from excited $F_H(CN^-)$ complexes into the isolated $CN^-$ defect system. We compare again (like in Fig. 2) vibrational emission[7] and anti-Stokes Raman spectra in this high $CN^-$ doped crystal, both excited around the $F_H(2)$ band maximum and measured at two low temperatures. The difference between the spectral results of the two techniques is very pronounced: In vibrational emission (measured only up to the $5\rightarrow4$ transition) a strong $v$-$v$ transfer from the $F_H$ center into isolated $CN^-$ defects appears already at 15 K, and increases strongly—by thermal activation—at 50 K. In contrast to this, our anti-Stokes Raman measurements show at 20 K exactly the same six-line spectrum of the $F_H(CN^-)$ transition as observed in the low-$CN^-$ doped crystal (Fig. 2) with no trace of any isolated $CN^-$ transition. Temperature increase to 50 K, which strongly increases the $v$-$v$ transfer, makes only a tiny signal of the free $CN^-$ $v=1\rightarrow0$ transition observable.

Evidently, for high $CN^-$ concentrations with strong $v$-$v$ transfer efficiency, ir emission and anti-Stokes Raman measurements yield very different spectral results and physical informations: In the ir technique $CN^-$ vibrational emission occurring in either the $F_H$ complex or isolated $CN^-$ defect appears with equal strength and cannot be separated. In the Raman technique the existent two types of transitions become nearly totally separated in strength by resonance Raman enhancement for the $F_H$ complex compared to an extremely weak—most likely off-resonance—Raman response of the isolated $CN^-$ defects.

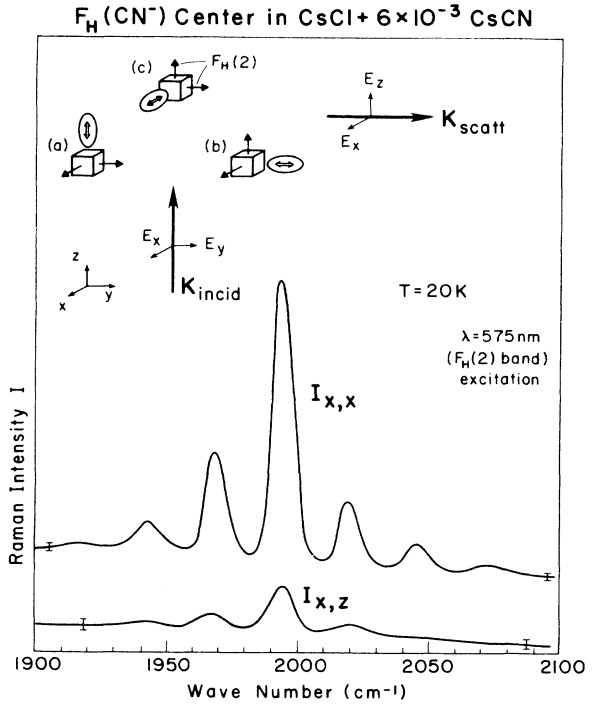


FIG. 6. Polarized anti-Stokes Raman spectra obtained under parallel $(x,x)$ and perpendicular $(x,z)$ polarization of incident and scattered light. The geometry of light propagation and polarization relative to the three perpendicular $F_H$ center orientations are schematically illustrated.

Polarization of Raman scattering is not easy to obtain in CsCl. Due to the fact that this material performs a NaCl→CsCl structural phase transition at 554 °C, the growth from the melt rarely yields single-crystal samples; additionally, the absence of cleaving along (100) planes makes it hard to identify crystal orientations. For the high-$CN^-$-doped crystal, we achieved by x-ray diffraction an approximate single crystal with the ⟨100⟩ direction defined within 9°. Figure 6 illustrates experimental geometry for this crystal with the (perpendicular) propagation vectors $K$ of the incident and scattered light along ⟨100⟩ directions of the crystal. The three orientations (a), (b), and (c) of the $F$-center–$CN^-$ pairs, present in equal amounts along the three ⟨100⟩ directions, are schematically illustrated too. Our use of $\lambda=575$ nm light excites only the $F_H(2)$ transitions perpendicular to the center axis so that $x$ polarized light will only excite centers (a) and (b) in Fig. 6. Stretching vibrations of the $CN^-$ neighbors with fixed orientations along the ⟨100⟩ pair axis do not change the symmetry of the defect: We therefore expect to observe anti-Stokes Raman scattering essentially polarized only parallel to the incident light. The experimental result shown in Fig. 6 confirms this expectation within the accuracy of crystal orientation.

In final experiments at 20 K with the high-$CN^-$-doped crystal, we used for the first time $\lambda=650$ nm pump light, exciting the $F_H(1)$ absorption transition parallel to the pair axis. Comparing the Raman spectra with the ones obtained under 532- and 650-nm excitation (perpendicular to the pair axis) yielded the following results.

(a) All three excitations produce Raman spectra with equal spectral positions and relative strength variation of the six lines. This is in agreement with the ir emission results[5] and thus confirm that in both $F_H(1)$ and $F_H(2)$ excitation cycles the same $e$-$v$ transfer and creation of population distribution in the excited $CN^-$ vibrational states occurs.

(b) In spite of considerably lower absorption strength at 650 nm compared to 575 nm, both excitations produce Raman spectra of about equal strength. This indicates that the Raman coupling between the excited electronic $p$ state and vibrational $CN^-$ state is stronger when both lie parallel [$F_H(1)$ band] compared to the perpendicular $F_H(2)$ case [see Fig. 1(a)].

(c) Experiments with ⟨100⟩ polarized $\lambda=650$ nm light yields the same result ($I_{x,x}\gg I_z$) as obtained for $\lambda=575$ nm excitation and illustrated in Fig. 6. As $x$-polarized light of the electronic transition parallel to the pair axis will only excite the pair orientation Fig. 6(c), we should again—for the same arguments as given above—observe Raman scattering polarized only parallel to the incident light polarization.

The most pronounced difference occurs under $\lambda=532$ nm excitation when comparing crystals with low ($7\times10^{-4}$) and high ($6\times10^{-3}$) $CN^-$ concentration but equal concentrations of $F_H(CN^-)$ pairs. While in the

low-doped crystal only a very small Raman signal at $-2080$ from free $CN^-$ defects are observable [Fig. 2(a)], the strength of this signal—relative to the $F_H(CN^-)$ spectrum—increases by at least a factor of 20 in the high-$CN^-$-doped crystal (the spectrum is not shown here). This confirms again—like ir emission results[5]—that the 2080-$cm^1$ signal is produced from excited $CN^-$ molecules in the $F_H(CN^-)$ pair by $v$-$v$ energy transfer into the free $CN^-$ molecule system, which should vastly increase in efficiency with $CN^-$ concentration. However, we can not yet decide if we are dealing with off-resonance Raman response of the totally free $CN^-$ defects, or with resonance Raman response of $CN^-$ defects in closer distance around the $F_H(CN^-)$ center, Raman-coupled to the latter by more diffuse electronic excited states of the $F_H$ center.

We regard this work as a first step and secure basis for new experimental approaches which are under way now to clarify the most interesting open questions. Instead of using the same laser-pulse for pumping and probing we will use spectrally different laser pulses of variable time delay for the two processes. The spectral separation will allow us to distinguish an off-resonance from a resonance scattering mechanism for the free $CN^-$ defects. Most importantly, the time delay between pump and probe pulse will allow us to determine with about 5 psec resolution the time scale for the two fundamental processes discussed: $e$-$v$ energy transfer inside the $F_H(CN^-)$ pair and $v$-$v$ energy transfer from the excited $F_H(CN^-)$ pair into the free $CN^-$ defect system.

An obvious question must still be answered: Why did we not measure the corresponding Raman spectra on the Stokes side of the spectrum, which should reveal by $\Delta v=1$ upward transitions the population of all excited $CN^-$ states relative to the $v=0$ ground state? The answer is simple but disturbing: Experiments involving both low- and high-$CN^-$-doped crystals showed under excitation with all three wavelengths an extremely intense background signal on the Stokes side (about $10^4$ times higher than the anti-Stokes Raman response). It consists of a very broad unstructured spectrum with a peak Stokes-shifted about 2500 $cm^{-1}$ from the laser line, totally burying the expected sharp line Raman spectrum of the $CN^-$ vibrations. The physical properties (like dependence on temperature, time-delay, excitation wavelength and intensity, etc.) are under present study to identify the origin and clarify the nature of this interesting but unknown Stokes signal.

## ACKNOWLEDGMENT

The work of one of us (F.L.) was supported in part by the National Science Foundation Grants No. DMR-82-11857 and DMR-87-06416. One of the authors (K.T.T.) would like to thank Faculty Grant-In-Aid Program of Arizona State University for partial support of this work. A Flinn Foundation Grant from Research Corporation is greatly appreciated.

[1]Y. Yang and F. Lüty, Phys. Rev. Lett. **51**, 419 (1983).
[2]L. Gomes and F. Lüty, Phys. Rev. B **30**, 7194 (1984).
[3]F. Lüty, Cryst. Lattice Defects Amorph. Mater. **12**, 343 (1985).
[4]D. J. Jang, T. C. Corcoran, M. A. El-Sayed, L. Gomes, and F. Lüty, *Ultrafast Phenomena V* (Springer-Verlag, Berlin, in press).
[5]Y. Yang, W. v. d. Osten, and F. Lüty, Phys. Rev. B **32**, 2724 (1985).
[6]W. Gellermann, Y. Yang, and F. Lüty, Optics Commun. **57**, 196 (1986).
[7]The shown vibrational emission data are spectra (recently measured by Y. Yang and F. Lüty) of improved resolution and sensitivity compared to the spectra published in Refs. 5 and 6.
[8]D. Y. Smith and G. Spinolo, Phys. Rev. **140**, A2121 (1965).
[9]D. S. Pan and F. Lüty, in *Light Scattering in Solids*, edited by M. Balkanski, R. C. C. Leite, and S. P. S. Porto (Flammarion, Paris, 1976), p. 277.
[10]D. Robbins and J. B. Page, Phys. Rev. Lett. **38**, 365 (1977).